PROCEEDINGS OF SCIENCE

SLAC-PUB-15491

$B \to X_{s/d}\gamma$ and $B \to X_{s/d}l^+l^-$

Martino Margoni[*†]
Universita' di Padova and INFN
E-mail: martino.margoni@pd.infn.it

Flavour Changing Neutral Current transitions $B \to X_{s/d}\gamma$ and $B \to X_{s/d}l^+l^-$ provide an excellent laboratory for the search for physics beyond the Standard Model and for the study of the dynamics of b-quark inside B mesons.
$B \to X_{s/d}\gamma$ and $B \to X_{s/d}l^+l^-$ decays are selected from the samples of events collected by the BaBar, Belle and CDF detectors by means of several strategies.
Standard Model tests are performed through measurements of inclusive $BR(B \to X_{s/d}\gamma)$, $BR(B \to X_{s/d}l^+l^-)$, CP and isospin asymmetries, and the study of the relevant angular distributions in $B \to X_{s/d}l^+l^-$ decays.
A $|V_{td}/V_{ts}|$ measurement with reduced theoretical uncertainties is obtained from the branching fraction ratio $BR(b \to d\gamma)/BR(b \to s\gamma)$.
The most precise $|V_{cb}|$ determination is extracted by global fits to the moments of inclusive distributions in $B \to X_c l\nu$ and $B \to X_s\gamma$ using the kinetic mass scheme. Uncertainties on shape functions in the measurement of $|V_{ub}|$ using inclusive semileptonic decays $B \to X_u l\nu$ are limited by comparing the partial rates for $B \to X_u l\nu$ and $B \to X_s\gamma$ in restricted phase space regions.

Kruger 2010: Workshop on Discovery Physics at the LHC
December 5 - 10, 2010
Kruger National Park, Mpumalanga, South Africa

*Speaker.
†On behalf of the BaBar Collaboration

Work supported in part by US Department of Energy under contract DE-AC02-76SF00515.

SLAC National Accelerator Laboratory, Menlo Park, CA 94025

1. Introduction

In the Standard Model, Flavour Changing Neutral Current transitions $B \to X_{s/d}\gamma$ occur via one-loop radiative penguin diagrams. Recent NNLL order computations give $BR(b \to s\gamma) = (3.15 \pm 0.23) \times 10^{-4}$ [1] for photons with Eγ>1.6 GeV in the B meson rest frame. Contributions from non Standard Model heavy particles in the loop can cause a sizeable deviation from the predicted rate. New physics can also significantly enhance the direct CP asymmetry for $b \to s\gamma$ and $b \to d\gamma$ decays which is $\sim 10^{-6}$ in the Standard Model [2].

The ratio $|V_{td}/V_{ts}|$ can be obtained both from the B_d and B_s mixing frequencies and from the study of the $B \to X_{s/d}\gamma$ transitions. A measurement of the branching fractions of inclusive $b \to d\gamma$ relative to $b \to s\gamma$ provides $|V_{td}/V_{ts}|$ with reduced theoretical uncertainties compared to that from the exclusive modes $B \to (\rho,\omega)\gamma$ and $B \to K^*\gamma$. It is important to confirm the consistency of the mixing and radiative decays measurements, since new physics effects would enter in different ways in the two processes.

Due to the universality of the b-quark motion inside B mesons, the moments of the photon spectrum in $B \to X_s\gamma$ decays are used to determine the Heavy Quark Expansion parameters related to the mass and momentum of the b-quark within the B meson. These parameters are useful to reduce the error in the determination of the CKM matrix elements $|V_{cb}|$ and $|V_{ub}|$ from the inclusive $B \to X_{c,u}l\nu$ decays [3], [4].

The lowest order Standard Model processes contributing to $B \to X_{s/d}l^+l^-$ are W^+W^- box and radiative photon or Z penguin diagrams. Their amplitudes are expressed using Operator Product Expansion in terms of hadronic form factors [5], and effective Wilson coefficients [6]. New particles in the loop could modify the Standard Model Wilson coefficients or introduce additional ones. The lepton forward-backward asymmetry, CP and isospin asymmetry, and the differential branching fraction in the decays $B \to X_{s/d}l^+l^-$ as functions of the dilepton invariant mass differ from the Standard Model expectations in various extended models [7].

2. $B \to X_{s/d}\gamma$ Measurements

2.1 Inclusive $B \to X_s\gamma$ Belle Analysis

From 605 fb^{-1} of data collected at the $\Upsilon(4S)$ resonance, events with a high energy isolated photon are selected [8]. Photons from π^0 and η decays are rejected exploiting informations about the electromagnetic shower profile, the two photons invariant mass and the photon angular distribution. The residual π^0/η $B\bar{B}$ background is estimated using data-corrected Monte Carlo samples and subtracted. The dominant background from continuum events is suppressed by means of two analysis streams, based respectively on a lepton tag and on energy flow and event shape variables. The residual amount of continuum background is subtracted using off-resonance data corrected for energy effects. The B meson is not reconstructed, therefore the $B \to X_d\gamma$ contribution is finally subtracted assuming $BR(B \to X_d\gamma)/BR(B \to X_s\gamma) = 4.5\%$. In the photon energy range from 1.7 to 2.8 GeV, as measured in the B meson rest frame, the partial branching fraction $BR(B \to X_s\gamma) = (3.45 \pm 0.15(stat) \pm 0.40(syst)) \times 10^{-4}$ is measured, where the systematic errors are dominated by the continuum and $B\bar{B}$ background subtraction.

PoS(Kruger 2010)048

2.2 Preliminary BaBar $B \to X_{s+d}\gamma$ Lepton Tag Analysis

From 347 fb^{-1} of data, events with an energetic photon are selected. Continuum background is suppressed using a lepton tag and a neural network exploiting topological event variables. $B\bar{B}$ background from $\pi^0/\eta,\omega$, electrons, anti-neutrons and final state radiation is estimated using simulation and data control samples and then subtracted. In the photon energy range from 2.1 and 2.8 GeV the CP asymmetry $A_{CP}(B \to X_{s+d}\gamma) = \frac{\Gamma(\bar{B}\to X_{s+d}\gamma)-\Gamma(B\to X_{s+d}\gamma)}{\Gamma(\bar{B}\to X_{s+d}\gamma)+\Gamma(B\to X_{s+d}\gamma)} = 0.056 \pm 0.060(stat) \pm 0.018(syst)$ is determined, where the B meson flavour is inferred from the lepton charge, taking into account the dilution due to mixing, cascade decays and fake leptons. This is the most precise measurement up-to-date, consistent with the Standard Model expectations. The statistical and systematic errors are dominated respectively by the continuum subtraction and the lepton tag asymmetry measured in data control samples.

2.3 Summary of $BR(b \to s\gamma)$ Measurements

The Heavy Flavour Averaging Group average of the inclusive $BR(b \to s\gamma)$ measurements for the summer 2010 conferences is $BR(b \to s\gamma) = (3.55 \pm 0.24(stat) \pm 0.09(syst)) \times 10^{-4}$ [9], in marginal agreement with the NNLL order theoretical prediction $BR(b \to s\gamma) = (3.15 \pm 0.23) \times 10^{-4}$ [1]. Recent calculations in the 2Higgs-Doublet-Model framework provide constraints on the coupling of the second and third generation fermions to the charged Higgs boson obtained from $BR(b \to s\gamma)$ together with other flavour physics experimental results. From these calculations, the current $\tan\beta$ independent best limit on the charged Higgs mass M_{H^+}>300 GeV/c^2 at 95% CL is obtained [10].

2.4 BaBar $|V_{td}/V_{ts}|$ Measurement

From 423 fb^{-1} of data, $b \to X_d\gamma$ and $b \to X_s\gamma$ inclusive rates are extrapolated from the sum of seven exclusive fully reconstructed modes with a high energy isolated photon [11]. The same kinematical cuts are applied to X_s and X_d states in order to reduce the systematics in the ratio of branching ratios. The dominant background from continuum is suppressed by means of a neural network using event shape variables. The contribution due to the missing states is estimated using Jetset Monte Carlo fragmentation models [12] corrected taking into account several measured exclusive decay modes [13].

In the hadronic mass region 0.5 GeV/c^2<M($X_{s/d}$)<2.0 GeV/c^2 the branching ratios measurements $BR(b \to s\gamma) = (230 \pm 8(stat) \pm 30(syst)) \times 10^{-6}$ and $BR(b \to d\gamma) = (9.2 \pm 2.0(stat) \pm 2.3(syst)) \times 10^{-6}$ are obtained. The unmeasured region M($X_{s/d}$)>2.0 GeV/c^2 is extrapolated using the spectral shape from the Kagan-Neubert model [14]. Conversion of the ratio of inclusive branching fractions to the ratio $|V_{td}/V_{ts}|$ is done according to [15] giving $|V_{td}/V_{ts}| = 0.199 \pm 0.022(stat) \pm 0.024(syst) \pm 0.002(th)$ where the systematic errors are dominated by the extrapolation to the inclusive rates. The theoretical error is strongly reduced compared to that from exclusive modes.

2.5 $B \to s\gamma$ Spectral Moments

The determination of $|V_{cb}|$ from the inclusive semileptonic decay $B \to X_c l \nu$ using Heavy Quark Effective Theory and Operator Product Expansion requires the non-perturbative parameters m_b and μ_π^2, representing the mass and the kinetic expectation value of the b-quark inside the B meson.

Combined fits in the kinetic mass scheme to the moments of the lepton momentum spectrum in $B \to X_c l \nu$ decays and of the photon energy spectrum in $B \to s\gamma$ decays provide the currently most precise $|V_{cb}|$ measurement $|V_{cb}| = (41.85 \pm 0.73) \times 10^{-3}$ [16].

The determination of $|V_{ub}|$ from the semileptonic branching ratio $BR(B \to X_u l \nu)$ requires shape functions to extrapolate the inclusive rate from the partial decay rates measured in restricted phase space regions with low background from $B \to X_c l \nu$. Due to the universality of b-quark motion inside B mesons, uncertainties on shape function are limited by comparing the partial rates for $B \to X_u l \nu$ and $B \to X_s \gamma$.

3. $B \to X_{s/d}l^+l^-$ Measurements

3.1 Belle $B \to K^{(*)}l^+l^-$ Analysis

From 605 fb^{-1} of data, $B \to K^{(*)}l^+l^-$ (with l=e or μ) events are fully reconstructed in ten different final states [17]. The dominant background from continuum is suppressed exploiting event shape variables. Semileptonic $B \to X l \nu$ decays are rejected by means of event shape, missing mass and lepton requirements. From the event yields in six $q^2 = m^2_{l^+l^-}$ bins, the differential branching fraction $\frac{dBR(B \to K^{(*)}l^+l^-)}{dq^2}$ is computed and compared to Standard Model predictions obtained using different assumpions on the decay form factors [18]. Figure 1 (left) shows the differential branching ratio separately for K$^*l^+l^-$ and Kl^+l^- final states.

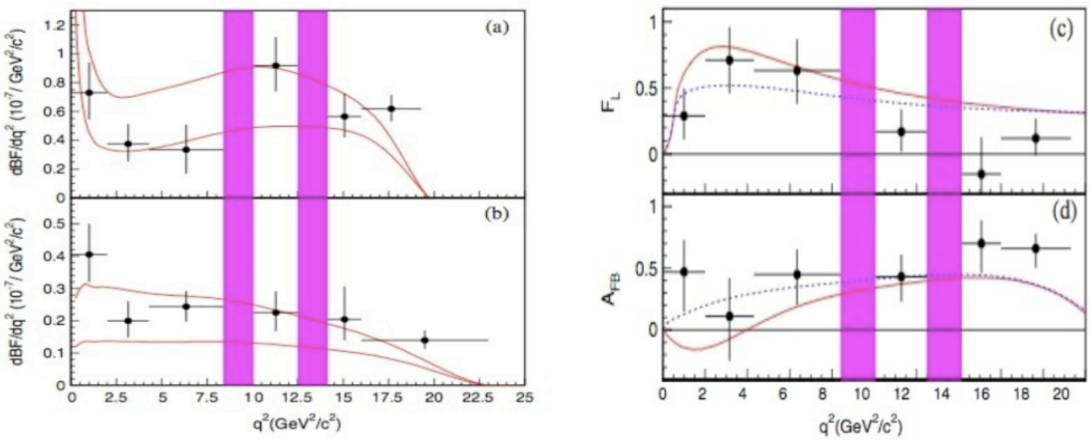

Figure 1: Differential branching ratios for the (a) K$^*l^+l^-$ and (b) Kl^+l^- modes as a function of q^2. The two shaded regions are veto windows to reject $J\Psi(\Psi')X$ events. The solid curves show the Standard Model theoretical predictions using different assumptions for the decay form factors. (c) and (d) show the fit results for F_L and A_{FB} in K$^*l^+l^-$ together with the solid (dotted) curve representing the Standard Model ($C_7 = -C_7^{SM}$) prediction.

The measured inclusive branching ratios $BR(B \to K^*l^+l^-) = (10.7 \pm^{1.1}_{1.0} \pm 0.9) \times 10^{-7}$, $BR(B \to Kl^+l^-) = (4.8 \pm^{0.5}_{0.4} \pm 0.3) \times 10^{-7}$, CP asymmetry $A_{CP} = \frac{N(B \to K^{(*)}l^+l^-) - N(\bar{B} \to K^{(*)}l^+l^-)}{N(B \to K^{(*)}l^+l^-) + N(B \to K^{(*)}l^+l^-)}$ and isospin asymmetry $A_I = \frac{(\tau_{B^+}/\tau_{B^0})BR(K^{(*)0}l^+l^-) - BR(K^{(*)\pm}l^+l^-)}{(\tau_{B^+}/\tau_{B^0})BR(K^{(*)0}l^+l^-) + BR(K^{(*)\pm}l^+l^-)}$ agree with the Standard Model expectations. Systematic errors are dominated by tracking, particle identification and Monte Carlo decay models.

PoS(Kruger 2010)048

The event angular distribution depends on three angles defined in figure 2. The K* longitudinal polarizarion fraction F_L and the forward-backward asymmetry A_{FB} are extracted from fits to $\cos\theta_{K^*}$ and $\cos\theta_l$ distributions,
$\frac{dN}{d\cos\theta_{K^*}} \sim \frac{3}{2}F_L\cos^2\theta_{K^*} + \frac{3}{4}(1-F_L)(1-\cos^2\theta_{K^*})$
and
$\frac{dN}{d\cos\theta_l} \sim \frac{3}{4}F_L(1-\cos^2\theta_l) + \frac{3}{8}(1-F_L)(1+\cos^2\theta_l) + A_{FB}\cos\theta_l$,
respectively. These quantites are sensitive to a sign-flip of the C_7 Wilson coefficient. Figure 1 (right) shows F_L and A_{FB} together with the Standard Model predictions for the two possible signs of C_7.

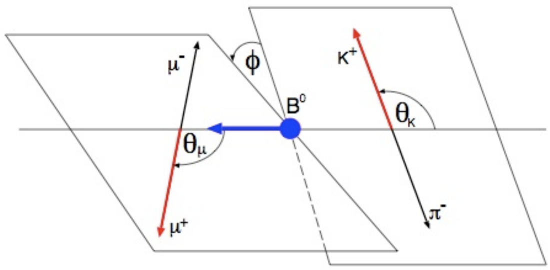

Figure 2: Definition of the relevant angles for the F_L and A_{FB} determination.

3.2 Preliminary CDF $B \to K\mu^+\mu^-$ Analysis

From 4.4 fb^{-1} of data, $B \to K^{(*)}\mu^+\mu^-$ events are fully reconstructed [19]. A dimuon trigger is applied exploiting lepton transverse momentum and $\mu^+\mu^-$ vertex informations. Signal events are selected using a neural network by means of event shape variables, vertex quality and lepton separation. In order to reduce the systematic error due to the efficiency estimation, the $B \to K\mu^+\mu^-$ branching ratio is computed relative to $B \to J/\Psi K^{(*)}$ which has identical final states. Results consistent with Standard Model expectations are obtained for inclusive and differential branching ratios, F_L and A_{FB}. The systematic errors are dominated by the combinatorial background description and $BR(B \to J/\Psi K^{(*)})$.

3.3 Preliminary BaBar $B^+ \to K^+\tau^+\tau^-$ Analysis

In some Standard Model extensions, such as NMSSM [20] the new physics couples proportionally to the mass squared of the decay products. In addition, the inclusive $B \to X_s\tau^+\tau^-$ branching ratio is expected to be comparable to $BR(B \to X_s l^+l^-)$ (with l=e or μ) in the high q^2 region and the exclusive $B^+ \to K^+\tau^+\tau^-$ transition is predicted to cover about 50% of the total inclusive rate. These arguments make the $B^+ \to K^+\tau^+\tau^-$ decay mode an important topic to be studied.

From 423 fb^{-1} of data, the BaBar Collaboration performs the first search for $B^+ \to K^+\tau^+\tau^-$ on the recoil of fully reconstructed $B \to D^{(*)}X$ decays. The dominant background from continuum events is suppressed exploiting the opening angle between the reconstructed B thrust and the rest-of-event thrust. Only one-prong $\tau \to e(\mu)\nu\nu, \pi\nu$ decays are reconstructed and di-tau candidates are selected in the three charged tracks topology. Background events are rejected based on missing energy and other kinematical quantities. From the 47 events surviving the cuts (with 65 expected from known backgrounds), the upper limit is obtained $BR(B^+ \to K^+\tau^+\tau^-) < 2.2 \times 10^{-3}$ at 90% CL. The dominant systematic errors are due to the signal efficiency computation and the background description.

4. Conclusions

The study of radiative penguin decays provides an excellent chance to search for new physics and to study the dynamic of b-quark inside B mesons. Almost all the results are in agreement with the expectations. In the future, the study of $B \to X_{s/d}\gamma$ and $B \to X_{s/d}l^+l^-$ transitions will offer the opportunity to improve the experimental techniques by using new angular observables with reduced dependence on form factors (e.g. Transversity Amplitudes) [21], perform very stringent Standard Model tests and, hopefully, to discover or to understand new physics.

References

[1] Misiak et al., Phys. Rev. Lett. 98, 022002.

[2] Hurt et al., hep-ph 0312260; hep-ph 0103331.

[3] Gambino et al., Eur. Phys. C 34, 181-189; Benson et al., Nucl. Phys. B 710, 371-401.

[4] Neubert et al., Phys. Rev. D 49, 4623-4633, Leibovich et al., Phys. Rev. D 61, 053006; Lange et al., JHEP10, 084.

[5] Bharucha et al., arXiv:1004.3249.

[6] Ali et al., Phys. Rev. D 61, 074024; Z. Phys. C 67, 417.

[7] Kruger et al., Phys. Rev. D 61, 114028; Phys. Rev. D 63, 019901(E); Aliev et al., Eur. Phys. J. C 29, 265; Hou et al., Phys. Rev. D 77, 014016.

[8] The Belle Collaboration, Phys. Rev. Lett. 103, 241801.

[9] The Heavy Flavour Averaging Group, http://www.slac.stanford.edu/xorg/hfag/rare/ichep10/radll/btosg.pdf.

[10] Mahmoudi et al., Phys. Rev. D 81, 035016.

[11] The BaBar Collaboration, Phys. Rev. D 82, 051101.

[12] T. Sjostrand, Comput. Phys. Commun. 82, 74.

[13] The BaBar Collaboration, Phys. Rev. D 72, 052005.

[14] Kagan and Neubert, Phys. Rev. D 58, 094012.

[15] Ali et al., Phys. Lett. B 429, 87.

[16] The Heavy Flavour Averaging Group, http://www.slac.stanford.edu/xorg/hfag/semi/EndOfYear09/gbl_fits/kinetic/index.html.

[17] The Belle Collaboration, Phys. Rev. Lett. 103, 171801.

[18] Ali et al., Phys. Rev. D 61, 074024; Phys. Rev. D 66, 034002.

[19] The CDF Collaboration, CDF Note 10047.

[20] Hiller and Gudrun, Phys. Rev. D 70, 034018.

[21] Bobeth et al., arXiv:1006.5013.